ChemPubSoc Europe

DOI: 10.1002/chem.201502475

CHEMISTRY A European Journal Full Paper

Kinase Inhibitors | *Hot Paper*

Design, Synthesis, and Biological Evaluation of Quercetagetin Analogues as JNK1 Inhibitors

Judith Hierold,[a] Sohee Baek ,[b, c, d] Rene Rieger,[a] Tae-Gyu Lim,[c] Saman Zakpur,[a] Marcelino Arciniega,[b] Ki Won Lee,[c, e] Robert Huber ,*[b, f, g, h] and Lutz F. Tietze*[a]

Abstract: The recent discovery of c-Jun NH_2-terminal kinase JNK1 suppression by natural quercetagetin (**1**) is a promising lead for the development of novel anticancer agents. Using both X-ray structure and docking analyses we predicted that 5′-hydroxy- (**2**) and 5′-hydroxymethyl-quercetagetin (**3**) would inhibit JNK1 more actively than the parent compound **1**. Notably, our drug design was based on the active enzyme–ligand complex as opposed to the enzyme's relatively open apo structure. In this paper we test our theoretical predictions, aided by docking-model experiments, and report the first synthesis and biological evaluation of quercetagetin analogues **2** and **3**. As calculated, both compounds strongly suppress JNK1 activity. The IC_{50} values were determined to be 3.4 μM and 12.2 μM, respectively, which shows that **2** surpasses the potency of the parent compound **1** (IC_{50} = 4.6 μM). Compound **2** was also shown to suppress matrix metalloproteinase-1 expression with high specificity after UV irradiation.

Introduction

The c-Jun NH_2-terminal kinases (JNKs) are serine/threonine protein kinases belonging to the mitogen-activated protein kinase family,[1] and they play a critical role in chronic diseases. JNKs have broad tissue distribution and are strongly activated by various inflammatory signals and stress stimuli. Although some debate exists regarding the exact role of JNKs in cancer, expression of JNK proteins is frequently altered in human tumors and cancer cells, including liver,[2] prostate,[3] and breast cancer.[4,5] In addition, JNKs are crucial mediators of obesity and insulin resistance, thus they are potential targets in type II diabetes.[6] Therefore, inhibition of JNKs is of considerable pharmaceutical relevance for cancer and other chronic diseases. Furthermore, matrix metalloproteinase-1 (MMP-1)—an interstitial collagenase that degrades extracellular matrix components[7]—is regulated by JNK signaling pathways[8] by modulating its expression through AP-1 (activator protein) transactivation.[9] JNK-activated AP-1 directly binds to human MMP-1 promoter and enhances MMP-1 transcription.[9] MMP-1 is an important player in UV-induced skin aging, thus it is a relevant pharmacological target and its activity may be suppressed by JNK inhibitors.

In a study aimed at identifying a novel small-molecule inhibitor of JNKs, we recently reported that the natural flavonoid quercetagetin[10] (**1**; Figure 1) strongly suppresses JNK1 activity.[11] Flavonoids are secondary plant metabolites showing a wide range of biological activities, including anti-inflammatory,[12] antiallergy, antifungal, antiviral, and antibacterial activities.[13] Consequently, both natural and synthetic flavonoids are frequently encountered in drug discovery.[14–20] In our hands, **1** inhibited JNK1 in an in vitro immobilized-metal-ion affinity-based fluorescence polarization (IMAP) assay with an IC_{50} value of 4.6 μM (Figure 2a).[11] Thus, it showed a higher activity than the pharmacological JNK1 inhibitor SP600125 (IC_{50} = 5.2 μM) (Figure 2b). Competitive-binding studies indicated that **1** occupies the ATP-binding site of JNK1 because the ATP concentration affected the level of inhibition exhibited by **1**. The func-

[a] *Dr. J. Hierold, R. Rieger, S. Zakpur, Prof. L. F. Tietze*
Institute for Organic and Biomolecular Chemistry
Georg-August-University Göttingen
Tammannstrasse 2, 37077 Göttingen (Germany)
Fax: (+49) 551-39-9476
E-mail: ltietze@gwdg.de

[b] *Dr. S. Baek , Dr. M. Arciniega, Prof. R. Huber*
Max-Planck-Institute for Biochemistry, Am Klopferspitz 18
82152 Martinsried (Germany)

[c] *Dr. S. Baek , Dr. T.-G. Lim, Prof. K. W. Lee*
Advanced Institutes of Convergence Technology, Seoul National University
Suwon 443-270 (Republic of Korea)

[d] *Dr. S. Baek*
Proteros Biostructures GmbH
Bunsenstr. 7a, 82152 Martinsried (Germany)

[e] *Prof. K. W. Lee*
WCU Biomodulation Major, Center for Food and Bioconvergence
Department of Agricultural Biotechnology, Seoul National University
Seoul (Republic of Korea)

[f] *Prof. R. Huber*
Department of Chemistry, Technical University of Munich
Lichtenbergstraße 4, 85748 Garching (Germany)

[g] *Prof. R. Huber*
Center for Medical Biotechnology
University of Duisburg-Essen, 45117 Essen (Germany)

[h] *Prof. R. Huber*
School of Biosciences, Cardiff University, Cardiff (Wales, UK)

Supporting information for this article is available on the WWW under http://dx.doi.org/10.1002/chem.201502475. It contains NMR spectra of all new compounds as well as a more detailed synthesis and characterization section.

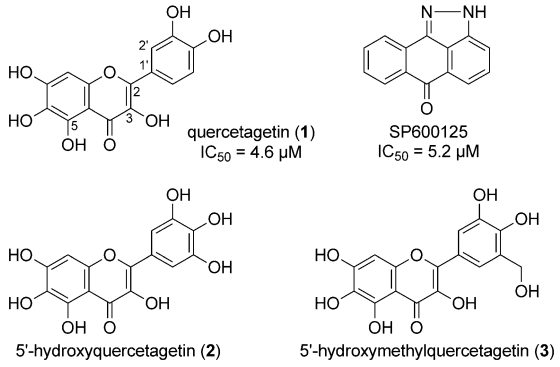

Figure 1. Verified and predicted small-molecule JNK1 inhibitors.

tional significance of the binding of **1** to JNK1 was examined in cell-based systems. The flavonoid was shown to strongly suppress UVB-induced phosphorylation of c-Jun, AKT, and GSK3β, as well as UVB-induced trans-activation of AP-1 and nuclear factor NF-κB. At a concentration of 5 μM, H-Ras-induced neoplastic cell transformation was inhibited by 73%. A two-stage mouse-skin-tumorgenesis model served to quantify the pharmacological effects. The flavonoid reduced tumor incidence in hairless mice by 46.7% following topical application at 20 nmol concentration, which indicated that **1** might be a suitable chemopreventive agent against UVB-mediated skin cancer.

The molecular basis of the inhibition of JNK1 by **1** was characterized by crystal-structure analysis of the JNK1–pepJIP1–**1** ternary complex (Figure 3).[11,21] Compound **1** is located in the ATP-binding site and forms a number of stabilizing hydrogen bonds with the protein. The binding of **1** results in significant structural changes of the apo-protein form through a hinge-bending motion.[11,22,23] The whole N-terminal lobe region is rotated towards the C-terminal lobe, which not only narrows, but also effectively caps the binding site after docking (Figure 3a). This feature improves compatibility of the ligand with the binding site of JNK1; compound **1** reaches much deeper into the ATP-binding site than SP600125.

A network of hydrogen bonds (Figure 3b) connects the catechol moiety with the side chains Lys55, Asp169, and Glu73, whereas the chromone portion forms hydrogen bonds with Glu109 and Met111.[24] Additional hydrophobic interactions between the ligand and the binding cleft further stabilize the structure. Notably, a water molecule trapped below the ligand participates in the hydrogen-bonding network by connecting the catechol moiety of **1** with Asp169 and Glu73. Its presence suggests that replacement of the trapped water molecules by an additional polar substituent on **1** might further increase the ligand selectivity and affinity. To test this hypothesis, we modeled the binding structure and affinity of **1** and appropriately modified derivatives by using different docking analyses.[11] The modeled docking poses of 5′-hydroxy- (**2**) and 5′-hydroxymethyl-quercetagetin (**3**) present an extra interaction with Asp169Oδ compared with the experimental pose of **1** (Figure 3c and d versus Figure 3b). Additionally, **3** is predicted to interact directly with Asp169N and Glu73Oε, in other words,

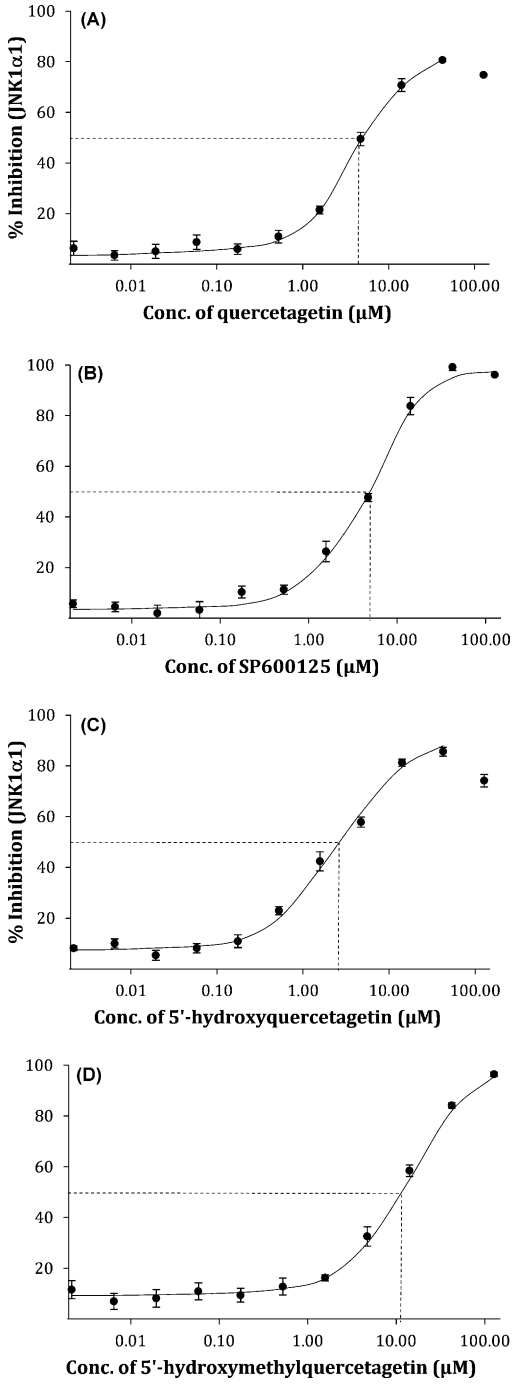

Figure 2. Inhibition of JNK1 (and the corresponding IC_{50} values) by A) **1**, B) SP600125, C) **2**, and D) **3** determined in an IMAP assay. The assay was performed as described in the Experimental Section. Each experiment was performed in triplicate. The data points for the titrations of **1** and **2** above 100 μM are affected by limited solubility and are not included in the calculation and curve fitting.

without mediation by the water molecule (Figure 3d). The predicted binding of **3** suggested that key interactions can be made without coordination of the water molecule, although the hydroxymethyl group does not occupy exactly the same position.

The results of a competitive-docking analysis are represented as docking scores (Table 1),[11] which are semiquantitative

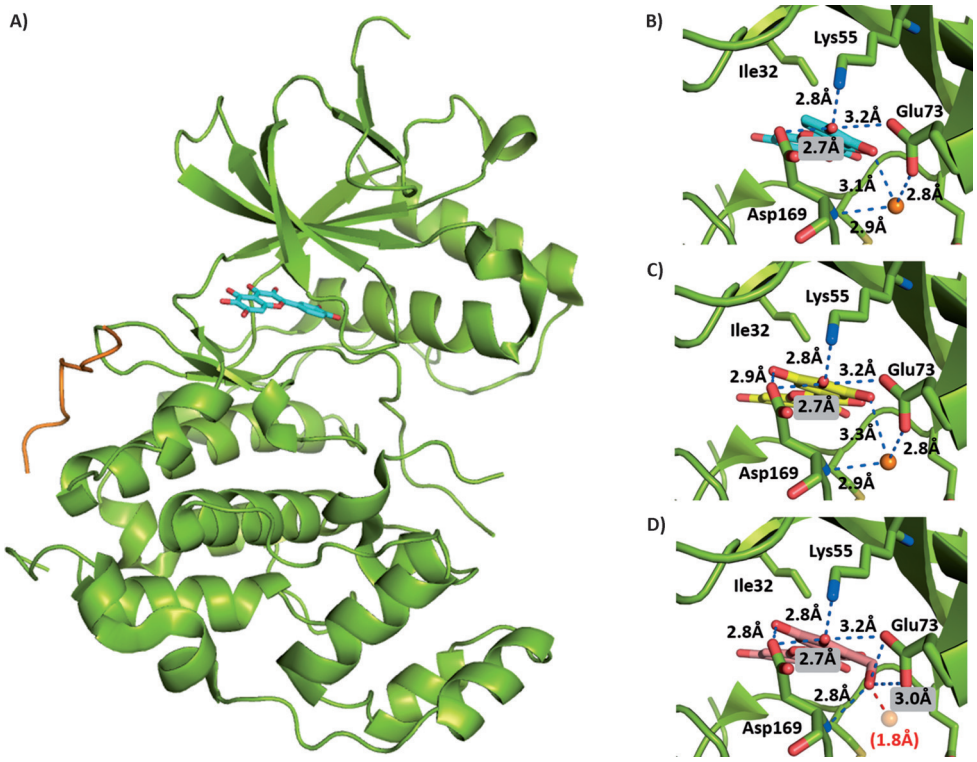

Figure 3. A) Crystal structure of the ternary JNK1(olive)–pepJP1(orange)–quercetagetin(blue) complex.[11] Comparison of the hydrogen-bond network between the B) experimental pose of **1** and the predicted binding poses of C) **2** and D) **3**. Hydrogen bonds are depicted as blue dashed lines. In the model of **3** the crystallographic water molecule is shown as a semitransparent sphere. It is unlikely to be present at this position and has not been considered in the modeling due to steric clashes (red dashed line, 1.8 Å).

Table 1. Evaluation of the binding affinity to JNK1 by docking analysis.[11]

Entry	Compound	H_2O mimic	Docking score[a]
1	SP600125[b]	–	−12.1
2	**1**	–	−12.5
3	**2**	–OH	−13.2
4	**3**	$–CH_2OH$	−14.1

[a] Docking score after incorporation into the conformation that JNK1 adopts after docking of **1** (activated form); [b] SP600125 is a pharmacological JNK1 inhibitor.

measures of the binding energy:[25,26] the lower the value, the stronger the binding affinity. In agreement with the higher biological activity of **1**, the docking score for **1** was lower than the score for SP600125 (−12.5 and −12.1, respectively). The calculations further indicated an improvement of the affinity for **2** and **3** with docking scores of −13.2 and −14.1, respectively.

In this paper we describe the first synthesis and biological evaluation of quercetagetin analogues **2** and **3**. As calculated, both compounds strongly inhibit JNK1. Gratifyingly, **2** surpasses the activity of the parent compound **1** with an IC_{50} value of 3.4 μM.

Results and Discussion

The synthesis of **2** commenced with a Claisen–Schmidt condensation of commercially available phenol **4** and benzaldehyde **5a** (Scheme 1) to give chalcone **6a** in 44% yield [76% based on recovered starting material (brsm)]. An intramolecular oxa-Michael addition yielded chromanone **7a**, which was subsequently oxidized to flavonol **9a** via the corresponding ketoxime. Compound **7a** was treated with isoamyl nitrite under acidic conditions to give ketoxime **8a**, which was hydrolyzed with sulfuric acid in acetic acid at reflux temperature to give to the desired flavonol **9a** in 68% over two steps. The traditional Algar–Flynn–Oyamada approach failed to yield the flavonol directly from chalcone **6a**, instead a competing α-addition provided aurone **10** in 13% yield. Global deprotection of **9a** with boron tribromide smoothly yielded

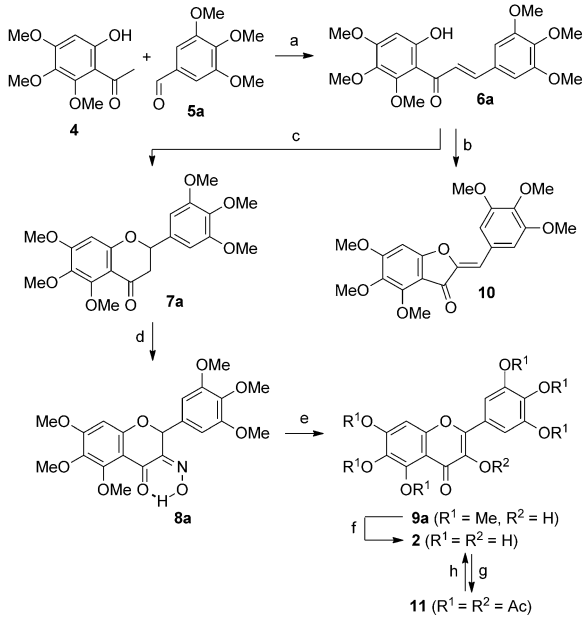

Scheme 1. Synthesis of **2**: a) NaOEt, EtOH, RT, 20 h, 44% (76% brsm); b) H_2O_2, NaOH (aq), MeOH, 0 °C to RT, 24 h, 13%; c) AcOH, 120 °C, 72 h, 54% (72% brsm); d) isoamyl nitrite, HCl, EtOH, 80 °C, 15 min; e) H_2SO_4, AcOH, 110 °C, 30 min, 68% (2 steps); f) BBr_3, CH_2Cl_2, 0 °C to RT, 16 h, then MeOH, 65 °C, 2 h, 99%; g) Ac_2O, cat. H_2SO_4, 0 °C to RT, 3 h, 98%; h) 6 M HCl, CH_3CN, 85 °C, 90 min, quant.

target compound **2**. Overall, **2** was prepared in 16% yield (37% brsm) over five consecutive steps.

The high polarity of **2** coupled with potential tautomerism to the 1,2-diketone impeded product purification by traditional methods. Whereas small quantities could be obtained by crystallization from ethyl acetate, on a larger scale it was more practical to purify the fully acetylated compound **11**. When **11** was exposed to hydrochloric acid in acetonitrile at reflux temperature the temporary acetyl groups were fully removed and highly pure **2** precipitated from the reaction mixture.

Benzaldehyde **5b**, required to access **2**, was prepared from commercially available 2,3-dihydroxybenzoic acid (**12**), which was regioselectively brominated, methylated, and reduced to give (5-bromo-2,3-dimethoxyphenyl)methanol (**14**) in 75% yield over three steps (Scheme 2). Compound **14** was subsequently silyl protected at the benzylic hydroxy group, which was followed by Stille cross-coupling with palladium tris(dibenzylideneacetone)dipalladium(0) ($[Pd_2(dba)_3]$), $P(tBu)_3$, cesium fluoride, and tributyl(vinyl)tin. The resultant styrene **15** then underwent a Lemieux–Johnson oxidation (osmium tetroxide and sodium periodate) to give the corresponding benzaldehyde. To ensure a high yield in the subsequent aldol condensation with phenol **4**, the bulky silyl protecting group was removed under standard conditions to yield benzaldehyde **5b**.

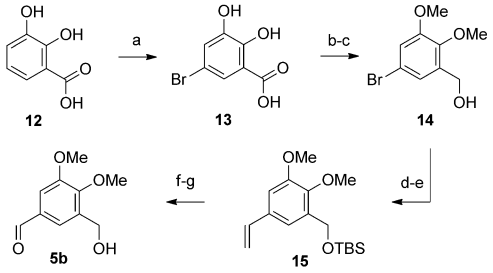

Scheme 2. Synthesis of **5b**: a) Br_2, AcOH, RT, 16 h, 99%; b) Me_2SO_4, K_2CO_3, acetone, 60 °C, 20 h, then NaOH (aq), MeOH, 70 °C, 2 h, 89%; c) BH_3·Me_2S, THF, RT, 16 h, 85%; d) TBSCl, imidazole, DMF, RT, 16 h, 89%; e) (vinyl)Sn(*n*Bu)$_3$, $[Pd_2(dba)_3]$ (1.5 mol%), $P(tBu)_3$ (6.0 mol%), CsF, dioxane, 102 °C, 16 h, 86%; f) OsO_4, $NaIO_4$, THF, H_2O, RT, 1 h, 62%; g) tetrabutylammonium fluoride (TBAF), THF, RT, 16 h, 98%.

Claisen–Schmidt condensation with phenol **4** resulted in chalcone formation in 73% yield (Scheme 3). Intramolecular oxa-Michael addition with concomitant acetylation of the benzylic alcohol furnished chromanone **7b**, which was oxidized with isoamyl nitrite as detailed above. Lewis acid cleavage of the ether C–O bonds furnished the intermediate alkoxyborane, which was hydrolyzed in water at reflux temperature to yield the target compound **3**. Performing the hydrolysis in methanol, which was successful for **9a**, led to methylation of the benzylic hydroxy group in the case of **9b**, therefore this method was unsuitable for formation of **3**. Purification of the flavonoid again proved challenging, and only approximately 90% purity of **3** was reached after repeated washing processes.

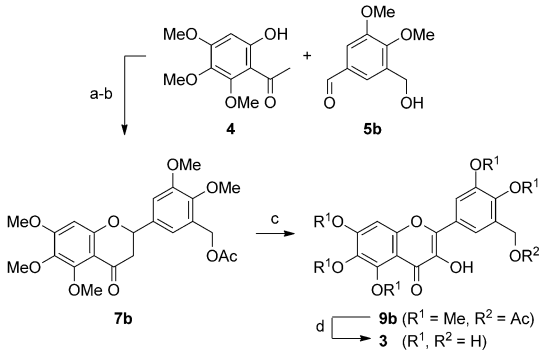

Scheme 3. Synthesis of **3**: a) NaOEt, EtOH, RT, 20 h, 73%; b) AcOH, 120 °C, 72 h, 56% (84% brsm); c) isoamyl nitrite, HCl, EtOH, 80 °C, 15 min, then H_2SO_4, AcOH, 110 °C, 30 min, 20%; d) BBr_3, CH_2Cl_2, 0 °C to RT, 16 h, then H_2O, 100 °C, 2 h, 97% (≈90% purity).

With both target molecules in hand we evaluated their biological performance. Theoretical modeling and docking-score calculations indicated an improvement of the affinity of **2** and **3** with docking scores of −13.2 and −14.1, respectively, compared to −12.5 for **1**. The IC_{50} values were calculated by using the IMAP assay system.[27] The IC_{50} values for **2** and **3** were determined to be 3.4 μM (Figure 2c) and 12.2 μM (Figure 2d), respectively.[28]

The obtained values indicate strong inhibition of JNK1, with **2** surpassing the inhibition of both the natural product (4.6 μM) and the pharmacological JNK1 inhibitor SP600125 (5.2 μM). Thus, our predictions based on the docking analysis held true for **2**, whereas hydroxymethyl-substituted inhibitor **3** proved to be less effective than predicted. These findings show that although theoretical calculations are indeed helpful, they must always be assessed by laboratory experimentation. The docking scores were very similar throughout the flavonoid series and a detailed ranking based solely on the scores must be viewed cautiously. The lower activity exhibited by **3** might indicate that the water molecule thought to be replaced by the 5′-hydroxymethyl substituent may play a more-specific role than expected.

Because **2** performed satisfactorily in the IMAP assay we further evaluated its biological profile. JNK1 plays a critical role for UV-induced MMP-1 expression by activating AP-1, a crucial transcription factor of MMP-1.[29] Thus, we investigated the activity of **2** on solar UV light (sUV) induced MMP-1 expression relative to the parent compound **1**. At the concentrations investigated in this study neither compound showed any significant cytotoxicity (Figure 4a). In line with previous reports,[30] sUV enhances MMP-1 expression in normal human dermal fibroblasts (NHDFs). Interestingly, our studies showed that **2** dramatically suppressed sUV-induced MMP-1 expression with a much-stronger activity than **1**, which had almost no effect in comparison (Figure 4b). However, because the JNK1 binding affinities of **1** and **2** are very similar other components of the JNK signaling pathway may play an essential role, which demands further study.

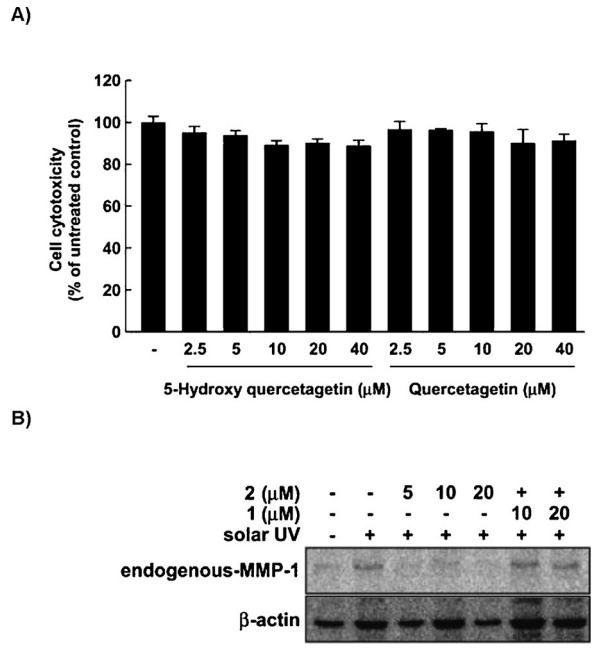

Figure 4. A) Inhibitors **2** and **1** show no significant cytotoxicity in NHDFs. The cells were cultured to confluence in 96-well plates, then treated with inhibitor for 24 h. Cytotoxicity was analyzed by using an MTS solution as indicated in the Experimental Section. Data are representative of three independent experiments that gave similar results. B) Inhibitor **2** shows a much-stronger inhibitory effect than **1** on sUV-induced MMP-1 expression. The cells were chemically treated for 1 h, then irradiated with sUV . After 36 h of exposure, the cells were disrupted with a lysis buffer. The MMP-1 protein was evaluated by using Western blot analysis as described in the Experimental Section. Data are representative of three independent experiments that gave similar results.

Conclusion

The development of clinically useful small-molecule kinase inhibitors has been a seminal event in the world of chronic diseases. Thus, the discovery of JNK1 suppression by natural product **1** was a promising lead in the development of novel anticancer agents. Based on X-ray structure and docking analyses we predicted that **2** and **3** would inhibit JNK1 more actively than the parent compound **1**. In this paper we evaluated our theoretical predictions and reported the first synthesis of derivatives **2** and **3**. Both analogues suppress JNK1 activity: compound **2** ($IC_{50}=3.4$ μM) surpassed the potency of **1** ($IC_{50}=4.6$ μM). Conversely, **3** showed a comparatively high IC_{50} value (12.2 μM), despite having the lowest docking score of the series in the theoretical calculations. The lower affinity of **3** in the experimental binding assay suggests that the water molecule present in the substrate–JNK1 complex may play a more specific structural role than expected. Cell biological experimentation showed that **2** exhibits very high specificity in suppressing MMP-1 expression after UV irradiation, and thus could impact skin aging.

Experimental Section

Compound 2

BBr_3 (1 M in CH_2Cl_2, 3.0 mL, 3.0 mmol, 15 equiv) was added via syringe pump over 15 min to a mechanically stirred solution of **9a** (84 mg, 0.20 mmol, 1.0 equiv) in dry CH_2Cl_2 (10 mL) at 0 °C. The resultant clear, orange solution was warmed to RT and stirred for 16 h during which time an orange solid precipitated. The reaction mixture was cooled to 0 °C and dry MeOH (10 mL) was added dropwise. The resultant clear solution was heated at 65 °C for 2 h, then cooled to RT. The volatile compounds were removed under reduced pressure. The resultant orange solid was suspended in H_2O (10 mL) and sonicated for 20 min. The suspension was left standing overnight and then carefully decanted. Recrystallization of the residue from EtOAc yielded **2** as a mustard-yellow solid (66 mg, 99%). ^{1}H NMR (600 MHz, [D_6]DMSO): $\delta=6.46$ (s, 1H; 8-H), 7.20 (s, 2H; 2′-H), 8.68 (brs, 2H; OH), 9.11 (brs, 3H; OH), 10.41 (brs, 1H; OH), 12.23 ppm (s, 1H; 3-OH); ^{13}C NMR (125 MHz, [D_6]DMSO): $\delta=93.01$ (C-8), 103.20, 107.09 (C-2′), 121.00, 128.45, 135.36, 135.66, 145.64 (C-3′), 145.84, 146.62, 148.73, 153.51, 175.68 ppm (C-4); IR: $\tilde{\nu}=3351$, 1666, 1607, 1561, 1538, 1504, 1474, 1312, 1274, 1207, 1167, 1100, 1045, 1023, 979, 821 cm^{-1}; UV/Vis (DMSO): λ_{max} (log ε) = 378 nm (4.2098); MS (ESI+): *m/z* (%): 335.0 (25) $[M+H]^+$, 357.0 (21) $[M+Na]^+$; MS (ESI−): *m/z* (%):333.0 (100) $[M-H]^-$; HRMS (ESI−): *m/z* calcd for $C_{15}H_{10}O_9$: 333.0252 $[M-H]^-$; found: 333.0249.

Compound 3

BBr_3 (1 M in CH_2Cl_2, 489 μL, 489 μmol, 15 equiv) was added via syringe pump over 15 min to a mechanically stirred solution of **9b** (15.0 mg, 32.6 μmol, 1.0 equiv) in dry CH_2Cl_2 (2 mL) at 0 °C. The resultant light-brown solution was warmed to RT and stirred for 16 h. The reaction mixture was cooled to 0 °C and H_2O (2 mL) was added dropwise. The resultant clear solution was heated at 80 °C for 2 h and then cooled to RT. The volatile compounds were removed under reduced pressure. The resultant brown solid was suspended in H_2O (10 mL) and sonicated for 20 min. The suspension was left to stand overnight and then carefully decanted to yield **3** as a beige solid (11 mg, 97%, purity ≈ 90%). ^{1}H NMR (300 MHz, CD_3OD): $\delta=4.73$ (s, 2H; CH_2), 6.51 (s, 1H; 8-H), 7.73 ppm (s, 2H; 2′-H and 6′-H); MS (ESI+): *m/z* (%): 349.1 (3) $[M+H]^+$, 371.0 (8) $[M+Na]^+$; HRMS (ESI−): *m/z* calcd for $C_{16}H_{12}O_9$: 347.0409 $[M-H]^-$; found: 347.0420.

Compound 9a

Conc. HCl (2 mL) was added via syringe pump over 10 min to a mechanically stirred solution of **7a** (781 mg, 1.9 mmol, 1.0 equiv) and isoamyl nitrite (1.56 mL, 11.6 mmol, 6.0 equiv) in dry ethanol (70 mL) at 0 °C. The reaction was stirred at 80 °C for 15 min. After cooling to RT the volatile compounds were evaporated under reduced pressure. The residue was taken up in EtOAc (60 mL) and washed with H_2O (2×50 mL). The combined aqueous layers were extracted with EtOAc (2×50 mL) and $CHCl_3$ (2×50 mL). The combined organic layers were washed with brine (80 mL), dried over $MgSO_4$, and concentrated under reduced pressure to yield the intermediate oxime as a yellow solid. The oxime was dissolved in glacial acetic acid (80 mL), cooled to 0 °C, and treated with 10% aqueous H_2SO_4 (16 mL). The reaction was stirred at 110 °C for 30 min, then cooled to RT, and concentrated under reduced pressure. The residue was taken up in EtOAc (70 mL) and washed with H_2O (2×50 mL). The combined aqueous layers were extracted with EtOAc (2×50 mL) and $CHCl_3$ (2×50 mL). The combined organic

layers were washed with brine (100 mL) and dried over $MgSO_4$. Evaporation of the volatile compounds gave the crude product, which was first purified by flash column chromatography (MeOH/CH_2Cl_2 = 1:19). The resultant highly fluorescent beige solid was suspended in EtOAc (5 mL) and carefully decanted to leave pure **9a** (543 mg, 68%) as a pale-beige solid. R_f = 0.41 (MeOH/CH_2Cl_2 = 1:19); ^{1}H NMR (600 MHz, $CDCl_3$): δ = 3.91 (s, 6H; 2×OMe), 3.95 (s, 6H; 2×OMe), 3.99 (s, 3H; OMe), 4.02 (s, 3H; OMe), 6.76 (s, 1H; 8-H), 7.39 (br s, 1H; 3-OH), 7.46 ppm (s, 2H; 2′-H); ^{13}C NMR (125 MHz, $CDCl_3$): δ = 56.4, 56.5, 61.0, 61.5, 62.2, 96.0, 105.1, 109.8, 126.4, 137.9, 139.8, 140.1, 142.1, 151.9, 153.3, 153.8, 158.5, 171.8 ppm; IR: $\tilde{\nu}$ = 3256, 2938, 2839, 1606, 1579, 1507, 1482, 1467, 1428, 1416, 1389, 1365, 1349, 1262, 1244, 1216, 1182, 1163, 1126, 1081, 1040, 994, 926, 850, 809, 770, 738, 694, 635, 568, 549, 531 cm^{-1}; UV/Vis (CH_3CN): λ_{max} (logε) = 214 (4.7864), 264 (4.2382), 346 nm (3.5254); MS (ESI+): *m/z* (%): 419.1 (100) $[M+H]^+$, 447.1 (14) $[M+Na]^+$, 859.2 (66) $[2M+Na]^+$, 1277.4 (21) $[3M+Na]^+$; HRMS (ESI+): *m/z* calcd for $C_{21}H_{22}O_9$: 419.1342 $[M+H]^+$; found: 419.1335.

Compound 11

A mechanically stirred suspension of **2** (100 mg, 0.30 mmol, 1.0 equiv) in acetic anhydride (10 mL) was degassed, cooled to 0 °C, and carefully treated with three drops of conc. H_2SO_4. After 15 min the solution turned clear and stirring was continued at RT for 3 h. H_2O (15 mL) was added at 0 °C, the mixture was diluted with EtOAc (20 mL), and the layers were thoroughly mixed by vigorous stirring at RT for 15 min. The layers were separated and the aqueous layer was extracted with EtOAc (2×20 mL). The combined organic layers were washed with H_2O (25 mL), dried over $MgSO_4$, and concentrated under reduced pressure. Purification by flash column chromatography (MeOH/CH_2Cl_2 = 1:49) yielded **11** as a pale-yellow solid (184 mg, 98%). R_f = 0.67 (MeOH/CH_2Cl_2 = 1:19); ^{1}H NMR (300 MHz, $CDCl_3$): δ = 2.32 (s, 6H; 2×OAc), 2.33 (s, 6H; 2×OAc), 2.34 (s, 3H; OAc), 2.36 (s, 3H; OAc), 2.43 (s, 3H; OAc), 7.48 (s, 1H; 8-H), 7.60 ppm (s, 2H; 2′-H and 6′-H); ^{13}C NMR (125 MHz, $CDCl_3$): δ = 20.02, 20.15, 20.36, 20.65, 20.69, 20.77, 110.29, 115.38, 120.77, 127.04, 132.97, 133.98, 136.87, 142.25, 143.62, 147.29, 153.24, 153.33, 166.49, 166.77, 167.05, 167.41, 167.84, 168.05, 169.83 ppm; IR: $\tilde{\nu}$ = 2930, 1770, 1656, 1628, 1499, 1461, 1423, 1370, 1354, 1166, 1141, 1051, 1012, 896, 870, 824, 693 cm^{-1}; UV/Vis (CH_3CN): λ_{max} (logε) = 253 (4.3279), 294 nm (4.2779); MS (ESI+): *m/z* (%): 629.1 (38) $[M+H]^+$, 651.1 (75) $[M+Na]^+$, 1279.2 (100) $[2M+Na]^+$; HRMS (ESI+): *m/z* calcd for $C_{29}H_{24}O_{16}$: 629.1137 $[M+H]^+$; found: 629.1115; HRMS (ESI+): *m/z* calcd for $C_{29}H_{24}O_{16}Na$: 651.0947 $[M+Na]^+$; found: 651.0957.

Compound 5b

A solution of TBS-protected alcohol **16** (see the Supporting Information; 310 mg, 1.0 mmol, 1.0 equiv) and TBAF (1 M in THF, 2.0 mL, 2.0 mmol, 2.0 equiv) in dry THF (15 mL) was stirred at RT for 16 h. 1 M aqueous HCl (5 mL) was added and the mixture extracted with EtOAc (5×20 mL). The combined organic layers were washed with brine (25 mL), dried over $MgSO_4$, and concentrated under reduced pressure. Purification by flash column chromatography (EtOAc/petroleum ether (PE) = 3:7→1:1) yielded **5b** as a white solid (192 mg, 98%). R_f = 0.14 (EtOAc/PE = 3:7); ^{1}H NMR (300 MHz, $CDCl_3$): δ = 2.75 (br s, 1H; OH), 3.89 (s, 3H; OMe), 3.93 (s, 3H; OMe), 4.72 (s, 2H; CH_2), 7.36 (d, J = 1.9 Hz, 1H; 6-H), 7.48 (d, J = 1.9 Hz, 1H; 2-H), 9.83 ppm (s, 1H; CHO); ^{13}C NMR (125 MHz, $CDCl_3$): δ = 56.2 (OMe), 61.0 (CH_2), 61.2 (OMe), 110.5 (C-6), 124.9 (C-2), 132.4 (C-1), 134.9 (C-3), 152.2 (C-4), 152.9 (C-5), 191.1 ppm (CHO); IR: $\tilde{\nu}$ = 3422, 2937, 1686, 1587, 1299, 1136, 999, 728 cm^{-1}; UV/Vis (CH_3CN): λ_{max} (logε) = 209 (4.2554), 223 (4.2263), 270 (3.9929), 308 nm (3.6603); MS (ESI+): *m/z* (%): 197.1 (100) $[M+H]^+$, 219.1 (91) $[M+Na]^+$; HRMS (ESI+): *m/z* calcd for $C_{10}H_{12}O_4$: 197.0808 $[M+H]^+$; found: 197.0808; HRMS (ESI+): *m/z* calcd for $C_{10}H_{12}O_4Na$: 219.0628 $[M+Na]^+$; found: 219.0628.

Compound 6b

A mechanically stirred solution of acetophenone **4** (580 mg, 2.95 mmol, 1.0 equiv) in dry EtOH (6 mL) was treated with a solution of NaOEt (1.02 g, 14.9 mmol, 5.0 equiv) in EtOH (20 mL), and the mixture was stirred at RT for 3 h. A solution of benzaldehyde **5b** (670 mg, 2.96 mmol, 1.0 equiv) in EtOH (16 mL) was added dropwise, and the resultant mixture was stirred at RT for 20 h. The solution was treated with H_2O (30 mL), acidified to pH 1 with 2.5 M aqueous HCl (20 mL), stirred for 10 min, and extracted with EtOAc (5×50 mL). The combined organic layers were washed with brine (1×100 mL), dried over $MgSO_4$, and concentrated under reduced pressure. Purification by flash column chromatography (EtOAc/PE = 3:7→1:1) yielded **6b** as an orange solid (870 mg, 73%). R_f = 0.2 (Et_2O/PE = 1:1); m.p. 114–119 °C; ^{1}H NMR (300 MHz, $CDCl_3$): δ = 2.25 (br t, J = 4.8 Hz, 1H; CH_2OH), 3.84 (s, 3H; OMe), 3.90 (s, 3H; OMe), 3.92 (s, 3H; OMe), 3.93 (s, 3H; OMe), 3.94 (s, 3H; OMe), 4.73 (br d, J = 4.8 Hz, 2H; CH_2OH), 6.30 (s, 1H; 3′-H), 7.12 (d, J = 2.0 Hz, 1H; 2-H), 7.28 (d, J = 2.0 Hz, 1H; 6-H), 7.77 (d, J = 15.6 Hz, 1H; H_α), 7.87 (d, J = 15.6 Hz, 1H; H_β), 13.67 ppm (br s, 1H; 2′-OH); ^{13}C NMR (125 MHz, $CDCl_3$): δ = 55.9, 56.1, 60.9, 61.2, 61.3, 61.9, 96.6, 108.7, 111.9, 121.1, 125.7, 131.3, 134.9, 135.3, 142.9, 148.8, 152.5, 154.9, 160.1, 162.6, 192.7 ppm; IR: $\tilde{\nu}$ = 2979, 2940, 1688, 1556, 1492, 1318, 1255, 1201, 1145, 1107, 1016, 987, 839, 811 cm^{-1}; UV/Vis (CH_3CN): λ_{max} (logε) = 209 (4.6730), 362 nm (4.3711); MS (ESI+): *m/z* (%): 405.2 (100) $[M+H]^+$, 831.3 (89) $[2M+Na]^+$, 1235.5 (67) $[3M+Na]^+$; HRMS (ESI+): *m/z* calcd for $C_{21}H_{24}O_8$: 405.1544 $[M+H]^+$; found: 405.1542.

Compound 7b

A mechanically stirred solution of chalcone **6b** (809 mg, 2.0 mmol, 1.0 equiv) in AcOH (120 mL) was heated at 120 °C for 72 h. The reaction was cooled to RT, treated with H_2O (50 mL), and extracted with EtOAc (3×100 mL). The combined organic layers were washed with brine (1×150 mL), dried over $MgSO_4$, and concentrated under reduced pressure. Purification by flash column chromatography (EtOAc/PE = 1:4→1:1) yielded **7b** as a yellow solid (500 mg, 56%). R_f = 0.65 (EtOAc/PE = 1:1); m.p. 114–118 °C; ^{1}H NMR (300 MHz, $CDCl_3$): δ = 2.11 (s, 3H; OAc), 2.77 (dd, J = 16.6, 2.9 Hz, 1H; 3-H_a), 3.01 (dd, J = 16.6, 13.4 Hz, 1H; 3-H_b), 3.83 (s, 3H; OMe), 3.877 (s, 3H; OMe), 3.880 (s, 3H; OMe), 3.91 (s, 3H; OMe), 3.94 (s, 3H; OMe), 5.17 (s, 2H; 3′-CH_2), 5.35 (dd, J = 13.4, 2.9 Hz, 1H; 2-H), 6.36 (s, 1H; 8-H), 7.00 (d, J = 2.1 Hz, 1H; 2′-H), 7.03 ppm (d, J = 2.1 Hz, 1H; 6′-H); ^{13}C NMR (125 MHz, $CDCl_3$): δ = 21.1, 45.7, 56.0, 56.2, 61.1, 61.4, 61.5, 61.7, 79.3, 96.4, 109.1, 110.4, 119.3, 130.1, 134.4, 137.6, 147.7, 152.8, 154.2, 159.4, 159.5, 170.6, 188.9 ppm; IR: $\tilde{\nu}$ = 2940, 2832, 1723, 1682, 1596, 1486, 1455, 1253, 1239, 1202, 1104, 1019, 998, 981, 857 cm^{-1}; UV/Vis (CH_3CN): λ_{max} (logε) = 276 (3.8903), 320 nm (3.7777); MS (ESI+): *m/z* (%): 447.2 (100) $[M+H]^+$, 469.2 (86) $[M+Na]^+$, 915.3 (92) $[2M+Na]^+$. HRMS (ESI+): *m/z* calcd for $C_{23}H_{26}O_9$: 447.1650 $[M+H]^+$; found: 447.1648; HRMS (ESI+): *m/z* calcd for $C_{23}H_{26}O_9Na$: 469.1469 $[M+Na]^+$; found: 469.1466.

Compound 9b

Conc. HCl (1 mL) was added via syringe pump over 10 min to a mechanically stirred solution of **7b** (500 mg, 1.12 mmol, 1.0 equiv)

and isoamyl nitrite (905 μL, 6.73 mmol, 6.0 equiv) in dry ethanol (35 mL) at 0 °C. The reaction was stirred at 80 °C for 15 min. After cooling the reaction mixture to RT, the volatile compounds were evaporated under reduced pressure. The residue was taken up in EtOAc (40 mL) and washed with H_2O (2×25 mL). The combined aqueous layers were extracted with EtOAc (2×25 mL) and $CHCl_3$ (2×25 mL). The combined organic layers were washed with brine (50 mL), dried over $MgSO_4$, and concentrated under reduced pressure to yield the intermediate oxime as a yellow solid. The oxime was dissolved in glacial acetic acid (40 mL), cooled to 0 °C, and treated with 10% aqueous H_2SO_4 (8 mL). The reaction was stirred at 110 °C for 30 min, then cooled to RT, and concentrated under reduced pressure. The residue was taken up in EtOAc (40 mL) and washed with H_2O (2×25 mL). The combined aqueous layers were extracted with EtOAc (2×25 mL) and $CHCl_3$ (2×25 mL). The combined organic layers were washed with brine (50 mL) and dried over $MgSO_4$. Evaporation of the volatile compounds gave the crude product, which was first purified by flash column chromatography (MeOH/CH_2Cl_2 = 1:19). The resultant dark-yellow solid (120 mg) was suspended in EtOAc (1 mL) and carefully decanted to leave pure **9b** (105 mg, 20%) as a light-yellow solid. R_f = 0.41 (MeOH/CH_2Cl_2 = 1:19); ^{1}H NMR (600 MHz, $CDCl_3$): δ = 2.11 (s, 3H; OAc), 3.91 (s, 3H; OMe), 3.93 (s, 3H; OMe), 3.96 (s, 3H; OMe), 3.99 (s, 3H; OMe), 4.01 (s, 3H; OMe), 5.22 (s, 2H; CH_2), 6.78 (s, 1H; 8-H), 7.34 (br s, 1H; 3-OH), 7.74 (d, J = 6.0 Hz; 1H), 7.85 ppm (d, J = 6.0 Hz; 1H); ^{13}C NMR (125 MHz, $CDCl_3$): δ = 21.26, 56.21, 56.60, 61.35, 61.73, 61.95, 62.37, 96.23, 109.87, 112.51, 121.27, 126.97, 129.98, 137.89, 140.16, 142.13, 149.17, 151.93, 152.73, 153.93, 158.54, 171.04, 171.82 ppm; IR: $\tilde{\nu}$ = 3281, 2942, 1737, 1728, 1607, 1481, 1261, 1215, 1162, 1082, 1017, 997 cm^{-1}; UV/Vis (CH_3CN): λ_{max} (logε) = 194 (4.6625), 252 (4.2698), 344 nm (4.2808); MS (ESI+): m/z (%): 461.2 (100) $[M+H]^+$, 921.3 (27) $[2M+H]^+$; HRMS (ESI+): m/z calcd for $C_{23}H_{24}O_{10}$: 461.1442 $[M+H]^+$; found: 461.1444.

IMAP assay

The IMAP assay was performed as previously described.[11] The IMAP assay was carried out with recombinant JNK1 (100 nM) in reaction buffer [3-(*N*-morpholino)propanesulfonic acid (MOPS) (20 mM; pH 6.5), dithiothreitol (DTT; 1 mM), $MgCl_2$ (10 mM), and polyoxyethyleneglycol dodecyl ether (Brij35; 0.01%)] in a 384-well black plate with serially diluted test compounds. A fluorescein-isothiocyanate-labeled JNK1 peptide substrate (LVEPLTPSGEAPNQK-5FAM-COOH) (400 nM) and ATP (7.46 μM) were added. After 60 min incubation with the potential inhibitor (5 μM) at RT, IMAP binding buffer (1:1200 dilution of IMAP progressive binding reagent in 65:35 IMAP progressive binding buffer A/IMAP progressive binding buffer B; supplied by Molecular Devices) was added and incubated for 60 min. The plate was read by using a PHERAstar Plus microplate reader (BMG Labtech). The excitation and emission wavelengths were λ = 485 nm (bandwidth = 20 nm) and λ = 530 nm (bandwidth = 25 nm), respectively.

Cell culture

NHDFs were purchased from the American Type Culture Collection (Manassas, VA, USA). NHDFs were cultured in DMEM</M199 (4:1 *v/v*) supplemented with fetal bovine serum (FBS; 10% *v/v*) at 37 °C under a 5% CO_2 atmosphere.

Cell cytotoxicity

The cell cytotoxicity of the compounds was evaluated with Cell Titer 96 AQueous One Solution (Promega). In brief, the cells were cultured in 96-well plates. Then, the NHDFs were starved with serum-free Dulbecco's modified eagle's medium (DMEM) for 24 h. The chemicals were added at the indicated concentrations. After 24 h, the MTS solution (20 μL) was added to each well and the plate was incubated for 1 h at 37 °C in the presence of 5% CO_2. The absorbance was analyzed at λ = 492 nm.

Western blot

The NHDFs were confluently cultured and starved with serum-free DMEM for 24 h. Chemicals were added to the cells for 1 h at the indicated concentrations. The cells were exposed to sUV light. After 36 h of sUV irradiation, the cells were lyzed with radio-immunoprecipitation assay (RIPA) buffer. Equal amounts of proteins were loaded onto 10% sodium dodecyl sulfate (SDS)/polyacrylamide gels and transferred to Immobilon P membranes (Millipore). The membrane was blocked with 5% fat-free milk for 1 h. The membrane was incubated with a specific primary antibody at 4 °C overnight. The proteins were hybridized with a horseradish peroxidase (HRP) conjugated secondary antibody, and the band was analyzed with a chemiluminescence detection kit (GE Healthcare, Pittsburgh, PA, USA).

Acknowledgements

This work was supported by the Deutsche Forschungsgemeinschaft (DFG), Land Niedersachsen, and Volkswagenstiftung. J.H. thanks the Dorothea-Schlözer Program for a postdoctoral scholarship.

Keywords: drug design · flavonoids · inhibitors · JNK1 · synthetic drugs

[1] B. Dérijard, M. Hibi, I.-H. Wu, T. Barrett, B. Su, T. Deng, M. Karin, R. J. Davis, *Cell* **1994**, *76*, 1025 – 1037.
[2] Q. Chang, Y. Zhang, K. J. Beezhold, D. Bhatia, H. Zhao, J. Chen, V. Castranova, X. Shi, F. Chen, *J. Hepatol.* **2009**, *50*, 323 – 333.
[3] X. Ouyang, W. J. Jessen, H. Al-Ahmadie, A. M. Serio, Y. Lin, W.-J. Shih, V. E. Reuter, P. T. Scardino, M. M. Shen, B. J. Aronow, A. J. Vickers, W. L. Gerald, C. Abate-Shen, *Cancer Res.* **2008**, *68*, 2132 – 2144.
[4] E. F. Wagner, A. R. Nebreda, *Nat. Rev. Cancer* **2009**, *9*, 537 – 549.
[5] T. Sakurai, S. Maeda, L. Chang, M. Karin, *Proc. Natl. Acad. Sci. USA* **2006**, *103*, 10544 – 10551.
[6] J. Hirosumi, G. Tuncman, L. Chang, C. Z. Görgün, L. T. Uysal, K. Maeda, M. Karin, G. S. Hotamisligil, *Nature* **2002**, *420*, 333 – 336.
[7] R. Visse, H. Nagase, *Circ. Res.* **2003**, *92*, 827 – 839.
[8] H. Endo, T. Watanabe, Y. Sugioka, M. Niioka, Y. Inagaki, I. Okazaki, *Int. J. Oncol.* **2009**, *35*, 1237 – 1245.
[9] C. Zugowski, F. Lieder, A. Mueller, J. Gasch, F. M. Corvinus, R. Moriggl, K. Friedrich, *Biol. Chem.* **2011**, *392*, 449 – 459.
[10] E. C. Bate-Smith, J. B. Harborne, *Phytochemistry* **1969**, *8*, 1035 – 1037.
[11] S. Baek, N. J. Kang, G. M. Popowicz, M. Arciniega, S. K. Jung, S. Byun, N. R. Song, Y.-S. Heo, B. Y. Kim, H. J. Lee, T. A. Holak, M. Augustin, A. M. Bode, R. Huber, Z. Dong, K. W. Lee, *J. Mol. Biol.* **2013**, *425*, 411 – 423.
[12] G.-J. Kang, S.-C. Han, J.-W. Ock, H.-K. Kang, E.-S. Yoo, *Biomol. Ther.* **2013**, *21*, 138 – 145.
[13] I. Duarte Silva, J. Gaspar, G. Gomes da Costa, A. S. Rodrigues, A. Laires, J. Rueff, *Chemico-Biol. Interactions* **2000**, *124*, 29 – 51.
[14] S. Holder, M. Zemskova, C. Zhang, M. Tabrizizad, R. Bremer, J. W. Neidigh, M. B. Lilly, *Mol. Cancer Ther.* **2007**, *6*, 163 – 172.
[15] D. Ichimatsu, M. Nomura, S. Nakamura, S. Moritani, K. Yokogawa, S. Kobayashi, T. Nishioka, K.-i. Miyamoto, *Mol. Carcinog.* **2007**, *46*, 436 – 445.
[16] C. Tsimplouli, C. Demetzos, M. Hadzopoulou-Cladaras, P. Pantazis, K. Dimas, *Eur. J. Nutr.* **2012**, *51*, 181 – 190.

[17] G.-J. Kang, S.-C. Han, N.-J. Kang, D.-H. Koo, D.-B. Park, S.-Y. Eun, H.-K. Kang, E.-S. Yoo, *Br. J. Dermatol.* **2014**, *171*, 512 – 523.
[18] Y. Jung, S. Y. Shin, Y. Yong, H. Jung, S. Ahn, Y. H. Lee, Y. Lim, *Chem. Biol. Drug Des.* **2015**, *85*, 574 – 585.
[19] K. Amrutha, P. Nanjan, S. K. Shaji, D. Sunilkumar, K. Subhalakshmi, L. Rajakrishna, A. Banerji, *Bioorg. Med. Chem. Lett.* **2014**, *24*, 4735 – 4742.
[20] E. Lee, K.-W. Jeong, H. N. Jnawali, A. Shin, Y.-S. Heo, Y. Kim, *Molecules* **2014**, *19*, 13200 – 13211.
[21] PepJIP1 is a docking-site peptide fragment of the scaffold protein JIP1.
[22] Y.-S. Heo, S.-K. Kim, C. I. Seo, Y. K. Kim, B.-J. Sung, H. S. Lee, J. I. Lee, S.-Y. Park, J. H. Wim, K. Y. Hwang, Y.-L. Hyun, Y. H. Jeon, S. Ro, J. M. Cho, T. G. Lee, C.-H. Yang, *EMBO J.* **2004**, *23*, 2185 – 2195.
[23] K. M. Comess, C. Sun, C. Abad-Zapatero, E. R. Goedken, R. J. Gum, D. W. Borhani, M. Argiriadi, D. R. Groebe, Y. Jia, J. E. Clampit, D. L. Haasch, H. T. Smith, S. Wang, D. Song, M. L. Coen, T. E. Cloutier, H. Tang, X. Cheng, C. Quinn, B. Liu, Z. Xin, G. Liu, E. H. Fry, V. Stoll, T. I. Ng, D. Banach, D. Marcotte, D. J. Burns, D. J. Calderwood, P. J. Hajduk, *ACS Chem. Biol.* **2011**, *6*, 234 – 244.
[24] For the importance of hydrogen-bond networks for kinase selectivity see: W. D. Jang, J.-T. Kim, N. S. Kang, *J. Mol. Liq.* **2014**, *191*, 37 – 41.
[25] R. A. Friesner, J. L. Banks, R. B. Murphy, T. A. Halgren, J. J. Klicic, D. T. Mainz, M. P. Repasky, E. H. Knoll, M. Shelley, J. K. Perry, D. E. Shaw, P. Francis, P. S. Shenkin, *J. Med. Chem.* **2004**, *47*, 1739 – 1749.
[26] R. A. Friesner, R. B. Murphy, M. P. Repasky, L. L. Frye, J. R. Greenwood, T. A. Halgren, P. C. Sanschagrin, D. T. Mainz, *J. Med. Chem.* **2006**, *49*, 6177 – 6196.
[27] J. R. Sportsman, E. A. Gaudet, A. Boge, *Assay Drug Dev. Technol.* **2004**, *2*, 205 – 214.
[28] For a theoretical calculation of the antioxidative properties of **2**, see: E. Estrada, J. A. Quincoces, G. Patlewicz, *Mol. Divers.* **2004**, *8*, 21 – 33.
[29] M. P. Vincenti, C. E. Brinckerhoff, *Arthritis Res.* **2002**, *4*, 157 – 164.
[30] T.-G. Lim, J.-E. Kim, S.-J. Lee, J. S. Park, M. H. Yeom, H. Chen, A. M. Bode, Z. Dong, K. W. Lee, *Int. J. Mol. Sci.* **2014**, *15*, 21419 – 21432.

Received: June 25, 2015
Published online on October 7, 2015